Physics of Plasmas

RESEARCH ARTICLE | JUNE 01 1995

A dispersion function for plasmas containing superthermal particles

R. L. Mace; M. A. Hellberg

Phys. Plasmas 2, 2098–2109 (1995)
https://doi.org/10.1063/1.871296

A dispersion function for plasmas containing superthermal particles

R. L. Mace and M. A. Hellberg
Plasma Physics Research Institute, Department of Physics, University of Natal, Durban, 4001, South Africa

(Received 26 September 1994; accepted 1 February 1995)

It is now well known that space plasmas frequently contain particle components that exhibit high, or superthermal, energy tails with approximate power law distributions in velocity space. Such nonthermal distributions, with overabundances of fast particles, can be better fitted, for supra- and superthermal velocities, by generalized Lorentzian or kappa distributions, than by Maxwellians or one of their variants. Employing the kappa distribution, with real values of the spectral index κ, in place of the Maxwellian we introduce a new plasma dispersion function expected to be of significant importance in kinetic theoretical studies of waves in space plasmas. It is demonstrated that this function is proportional to Gauss' hypergeometric function ${}_2F_1[1,2\kappa+2;\kappa+2;z]$ enabling the well-established theory of the hypergeometric function to be used to manipulate dispersion relations. The reduction, for integer values of κ, to the less general so-called modified plasma dispersion function [Phys. Fluids B **3**, 1835 (1991)] is demonstrated. An example illustrating the use of the function is presented.

I. INTRODUCTION

Kinetic theoretical studies of waves in space plasmas have, until recently, centered on the investigation of plasmas near thermal equilibrium, i.e., the lowest-order (or in quasi-linear theory, the spatially averaged) particle distribution functions have been *assumed* to be Maxwellians or one of their variants. In laboratory plasmas as well, the Maxwellian distribution has found much practical use as a model for the lowest-order particle distribution functions. Consequently the mathematics used to describe thermal or Maxwellian plasmas is well established and is based upon the well-known plasma dispersion, or Z function,[1]

$$Z(\xi)=\pi^{-1/2}\int_{-\infty}^{\infty}\frac{e^{-s^2}}{s-\xi}\,ds,\quad \mathrm{Im}(\xi)>0.$$

The use of the Maxwellian distribution—and the associated wave theory based on the Z function—in modeling the tenuous and largely collisionless plasmas found in space and astrophysics has occurred, despite the fact that they frequently exhibit constituent particle distribution functions that are far from their equilibrium Maxwellian or relativistic Maxwellian forms. Indeed, observation, either directly or by inference—such as inferring the particle properties from the radiative signatures of the plasma, as is often done in astrophysics—frequently suggests that particles whose energies exceed thermal energies obey a power law distribution in the particle energy, momentum, and velocity, e.g.,

$$4\pi v^2 f(v)dv\propto v^{-\alpha}\,dv,\quad \text{for } |v|>v_{\mathrm{th}}. \tag{1}$$

Examples of plasmas with particle distributions of the form (1) include solar flares;[2] the solar wind;[3] the galactic cosmic ray distribution;[4] and plasma in a superthermal radiation field,[5] amongst others. For an extensive list of plasmas containing particles with power law distributions, the reviews cited in the following paragraph may be consulted. In addition, recent kinetic particle-in-cell (PIC) simulations of plasma shock waves[6–9] have demonstrated the validity of (1) in the vicinity of collisionless shocks, entities that occur abundantly in the space and astrophysical environment. Recent studies related specifically to waves in nonthermal space plasmas include Refs. 10–12.

Physical mechanisms that lead naturally to power laws of the form (1) are the first- and second-order Fermi acceleration mechanisms (see Refs. 4, 13, and 14 for reviews). In first-order Fermi acceleration, high-energy particles are a natural byproduct of the passage of a collisionless shock wave. They are accelerated systematically by scattering off resonant plasma waves, such as Alfvén waves for the ions and whistlers for the electrons, as they "diffuse" through the shock front and encounter the converging flows on either side. The attractiveness of the Fermi mechanism is two-fold: (i) a particularly simple theory leads to particle distributions of the form (1) with the "spectral index," α, given by

$$\alpha=\frac{3u_1}{u_1-u_2}=\frac{3r}{r-1}, \tag{2}$$

where $r=u_1/u_2$ is the shock compression ratio, and u_1 and u_2 are the upstream and downstream bulk flow velocities, respectively; (ii) shocks are ubiquitous in space and astrophysics.

Second-order Fermi acceleration, or stochastic acceleration, is a less efficient process, but can nevertheless lead to particle distributions of the form (1). This process entails the damping of magnetohydrodynamic (MHD) turbulence by fast particles—the energy in the MHD turbulence being transferred to the fast particles.[15] Obviously the magnetoacoustic, as opposed to the Alfvén, component of the MHD turbulence will be the more effective in the acceleration process, as it is the more strongly damped. Electrons are most likely to resonate, initially, with whistlers, but they too can scatter on MHD waves when they attain sufficiently large momenta.

A point that we wish to stress here, and that was implied in the foregoing discussion, is that the spectral index, α, of the particle distributions (1) will, in general, be nonintegral. If we consider shock accelerated particles (the first-order Fermi mechanism), for example, then α given by (2) will, in

 1070-664X/95/2(6)/2098/12/$6.00

general, be a real value as the shock compression ratio, derivable from the Rankine–Hugoniot relations, is in general a real value. For strong shocks (first-order Fermi acceleration), however, we expect α to approach the integral value of 4 asymptotically.[15] For a plasma in a radiation field, Hasegawa *et al.*[5] present a formula [their Eq. (18)] for the velocity spectral index, α (κ in their notation), which depends on the Coulomb logarithm and the plasma Debye length, and is, in general, real valued.

Summers and Thorne[16] point out that a useful distribution for modeling a plasma containing suprathermal and superthermal particles is the generalized Lorentzian, or kappa, distribution:

$$f(v)=(\pi\kappa\theta^2)^{-3/2}\frac{\Gamma(\kappa+1)}{\Gamma(\kappa-\frac{1}{2})}\left(1+\frac{v^2}{\kappa\theta^2}\right)^{-(\kappa+1)}, \tag{3}$$

where θ is a *modified* thermal speed related to the usual thermal speed, $v_{\mathrm{th}}\equiv(T/m)^{1/2}$, by $\theta=[(2\kappa-3)/\kappa]^{1/2}\times(T/m)^{1/2}=[(2\kappa-3)/\kappa]^{1/2}v_{\mathrm{th}}$ when[16] $\kappa>\frac{3}{2}$. The normalization of f has been chosen such that $\int f(v)d^3v=1$. The kappa distribution reduces to the ordinary Lorentzian distribution for $\kappa=1$, and to the Maxwellian distribution for $\kappa\rightarrow\infty$. Summers and Thorne[16] introduced a new plasma dispersion function, Z_κ^*, based on (3), but they restricted κ to strictly integer values. In view of our earlier discussion, we do not impose the constraint that κ be an integer here.

The kappa distribution (3) indeed possesses the desired property that particles with velocities greater than the thermal velocity $v_{\mathrm{th}}\sim\theta$ obey a power law distribution of the form (1). Comparing (3) with (1) we notice immediately that $\alpha\simeq2\kappa$. Thus, in the first-order Fermi acceleration picture we would expect that particle distributions in the vicinity of a strong shock ($\alpha\simeq4$) should have κ close to, but less than 2.

Examples of plasmas whose particle velocity distributions can be described by (3) with *noninteger* spectral index κ occur in the Earth's plasma sheet and in the distant magnetotail, among others. Christon *et al.*[17] have observed during plasma sheet temperature transitions—periods (typically ~30–60 min) of low plasma bulk velocity when the plasma thermal energy either increases or decreases steadily—that the plasma sheet ion and electron velocity distributions can be well fitted by (3). For example, they found that a kappa distribution with $\kappa=4.7$ provided a good fit to plasma sheet ion data measured at 0549UT on day 169, 1978. On the other hand, at 1948UT on day 043, 1978 they found that $\kappa=5.5$ produced an excellent fit to the electron data. Christon *et al.*[17] further demonstrated the ability of the kappa distribution to provide a reasonable description of the nonthermal high-energy tails of magnetospheric plasma proton and helium spectra. Employing data observed in a fast-moving plasma structure in the distant ($\sim216R_{\mathrm{E}}$, where R_{E} is the Earth's radius) magnetotail, they found a good fit to the ion particle data could be obtained with the kappa distribution with $\kappa=5.5$.

In this paper we employ the definition of the kappa distribution (3) with real-valued spectral index κ, to define, analogously to the work of Summers and Thorne,[16] a plasma dispersion function, Z_κ, for plasmas containing supra- and superthermal particles. The function Z_κ offers a more complete description of waves in kinetic space plasmas than does the function Z_κ^* of Summers and Thorne[16] because it can model particle distributions whose spectral indices are nonintegral. It facilitates investigation of the subtle changes in the wave–particle dynamics brought about by finely varying κ, and thus the shape of the superthermal particle tail. We show that this dispersion function is closely related to Gauss' hypergeometric function for which there exists a well-established and extensive theory. By using the theory of the hypergeometric function, we derive various properties of Z_κ. In addition, we show the correspondence of Z_κ, for integer values of κ, with the function Z_κ^* of Summers and Thorne.[16] The geometrical properties of the function are briefly discussed and the function's use in a simple application is demonstrated.

It should also be mentioned that while we have used the form (3), which is valid for an isotropic plasma, other nonisotropic velocity distributions closely related to the kappa distribution can be constructed. These distributions are analogous to the loss-cone, bi-Maxwellian and "heat-flux" bi-Maxwellian distributions (see Table I of Ref. 16) usually found in thermal plasmas. The choice of which distribution function to use will obviously be dictated by the physical scenario under investigation. However, we have considered here the simplest case of an isotropic plasma to avoid unnecessary complications and to aid comparison with earlier work.[16] In general, though, if the distribution of velocities parallel to the ambient magnetic field, $v_\parallel$ can be described by $\propto(1+v_\parallel^2/\kappa\theta_\parallel^2)^{-(\kappa+1)}$ (where $\theta_\parallel$ is a modified parallel temperature analogous to θ in the previous paragraph) we would expect the dispersion function, Z_κ, discussed here, to play a role.

II. MATHEMATICAL DEVELOPMENT

We define the function $Z_\kappa(\xi)$ analogously to the function $Z_\kappa^*(\xi)$ as given in Summers and Thorne:[16]

$$Z_\kappa(\xi)=\frac{1}{\pi^{1/2}\kappa^{3/2}}\frac{\Gamma(\kappa+1)}{\Gamma(\kappa-\frac{1}{2})}Q(\xi), \tag{4}$$

where

$$Q(\xi)=\int_{-\infty}^{\infty}\frac{ds}{(s-\xi)(1+s^2/\kappa)^{\kappa+1}};\quad \mathrm{Im}(\xi)>0. \tag{5}$$

Here we do not constrain κ to be an integer as was done previously.[16]

The integral defining $Q(\xi)$ is recognizable as the Hilbert transform of the function $(1+s^2/\kappa)^{-(\kappa+1)}$, i.e., the kappa distribution in suitably normalized form, and is thus readily analytically continued to $\mathrm{Im}(\xi)\leqslant0$.

Summers and Thorne[16] proceeded to evaluate $Q(\xi)$ by closing the contour upward around the poles of the integrand, and so arrived at a terminating series representation for $Q(\xi)$, and hence $Z_\kappa(\xi)$. For arbitrary real κ a similar approach may be used (see the Appendix), except that, in general, the integrand of (5) now possesses singularities of the branch type. Indeed, the integrand has two branch points, namely $z=i\sqrt{\kappa}$ and $z=-i\sqrt{\kappa}$. With the standard definitions of arg(z) and Arg(z), i.e.,

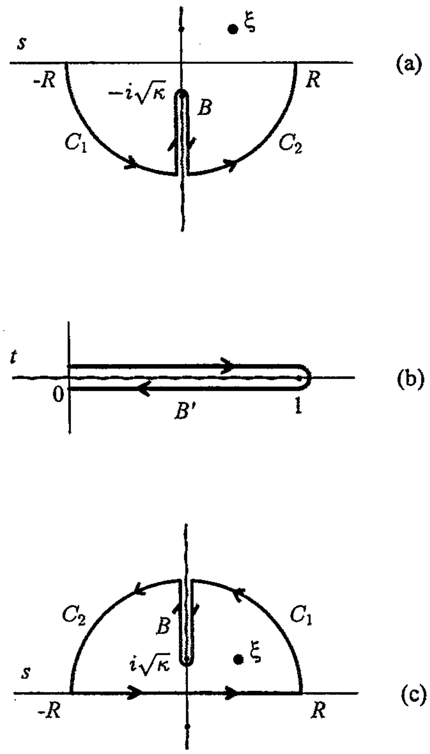

FIG. 1. Integration contours for the evaluation of Z_κ. (a) The original contour in the s plane used in Sec. II and (b) the equivalent transformed contour in the t plane. (c) The alternative contour of integration used in the Appendix. The wavy lines indicate branch cuts.

$$-\pi<\arg(z)\leq\pi;\quad \operatorname{Arg}(z)=\arg(z)+2k\pi,$$
$$k=0,\pm1,\pm2,\pm\cdots,$$

the branch lines can be chosen to extend from the points $i\sqrt{\kappa}$ and $-i\sqrt{\kappa}$ to $i\infty$ and $-i\infty$, respectively, along the imaginary axis. Thus, in closing the contour upward (or downward) one must ensure that it does not cross the branch line.

However, a simpler method, which immediately yields the correct analytic continuation for $Q(\xi)$, is to deform the contour along the real line, as illustrated in Fig. 1(a), downward into an anticlockwise, quarter-circular segment from $-\infty$ to $-\epsilon-i\infty$ (C_1), loop around the lower branch in a clockwise direction (B), and then proceed from $\epsilon-i\infty$ to ∞ along another anticlockwise quarter-circle (C_2). It is not difficult to verify that the integrals along the quarter-circles vanish in the limit $R\to\infty$, provided $\kappa>-1$. Beginning with the definition (5), we can therefore write

$$Q(\xi)=\int_B\frac{ds}{(s-\xi)(1+s^2/\kappa)^{\kappa+1}},\tag{6}$$

where B denotes that part of the contour encircling the branch cut. Now let us consider this integral under the transformation

$$t=\frac{2}{1-s/i\sqrt{\kappa}},\tag{7}$$

which yields

$$Q(\xi)=\frac{-1}{2^{2\kappa+2}}\int_{B'}t^{2\kappa+1}(t-1)^{-(\kappa+1)}\times\left[1-t\left(\frac{i\sqrt{\kappa}-\xi}{2i\sqrt{\kappa}}\right)\right]^{-1}dt,\tag{8}$$

where the subscript B' on the integral denotes the new contour [under the transformation (7)]. It is not difficult to see that the contour in the s plane encircling the point $s=-i\sqrt{\kappa}$ (B) becomes a loop extending from the point $t=0+0i$ around the point $t=1$ and back to $t=0-0i$, in a clockwise direction, in the t plane [see Fig. 1(b)]. The integrand in the above has a branch cut extending from $t=1$ to $t=-\infty$ along the x axis (actually, the integrand contains two branch cuts: one extending from 0 to $-\infty$; the other from 1 to $-\infty$). Consider now the integral

$$I=\int_{B'}t^{b-1}(t-1)^{c-b-1}(1-tz)^{-a}\,dt.\tag{9}$$

The integral in (8) is representable in this form if we put

$$a=1;\quad b=2\kappa+2;\quad c=\kappa+2;\quad z=\frac{i\sqrt{\kappa}-\xi}{2i\sqrt{\kappa}}.\tag{10}$$

We note, in particular, that a is an integer which results in some simplification, i.e., the additional branch point of the integrand at $t=1/z$ is removed.

Let us deform the contour B' onto the x axis; then

$$I=(e^{-i(c-b)\pi}-e^{i(c-b)\pi})\int_0^{1-\epsilon}t^{b-1}(1-t)^{c-b-1}\times(1-tz)^{-a}\,dt+\int_{C_\epsilon}t^{b-1}(t-1)^{c-b-1}(1-tz)^{-1}\,dt,\tag{11}$$

where C_ϵ is a small clockwise circle (radius ϵ) centered on the point $t=1$. Now, provided $c-b>0$, or equivalently, $\kappa<0$, the integral around C_ϵ vanishes. Thus, we have in the limit $\epsilon\to0$,

$$I=-2i\sin[(c-b)\pi]\int_0^1 t^{b-1}(1-t)^{c-b-1}\times(1-tz)^{-a}\,dt,\tag{12}$$

provided $c-b>0$. The integral on the right-hand side of (12) is Pochhammer's integral, which allows us to make the connection with Gauss' hypergeometric function. The hypergeometric function is defined in terms of Pochhammer's integral as follows:[18]

$${}_2F_1[a,b;c;z]=\frac{\Gamma(c)}{\Gamma(b)\Gamma(c-b)}\int_0^1 t^{b-1}(1-t)^{c-b-1}\times(1-tz)^{-a}\,dt,\tag{13}$$

which enables us to write (12) as

$$I=-2i\sin[(c-b)\pi]\,\frac{\Gamma(b)\Gamma(c-b)}{\Gamma(c)}\,{}_2F_1[a,b;c;z].\tag{14}$$

Equation (14) establishes the connection of the integral around the branch line with Gauss' hypergeometric function ${}_2F_1[a,b;c;z]$. Thus, using (8) and (10) we obtain the contribution from the branch,

$$Q(\xi)=\frac{2i}{2^{2\kappa+2}}\frac{\Gamma(2\kappa+2)\Gamma(-\kappa)\sin(-\kappa\pi)}{\Gamma(\kappa+2)}\times{}_2F_1[1,2\kappa+2;\kappa+2;\tfrac{1}{2}(1-\xi/i\sqrt{\kappa})]. \tag{15}$$

Note that we have derived Eqs. (14) and (15) under the assumption $c-b>0$, or equivalently $\kappa<0$. It is important to note, however, that the loop integrals around the branches (in the t or s planes) are well defined for all $c-b$ and κ as they do not pass through any singularities. Thus, we deduce that (15) holds for all $\kappa>-1$ (see our earlier convergence criterion) except those integer κ for which one of the Γ functions in the numerator diverges. We can remove the singularities for positive, integer κ using the reflection formula for the Γ function,

$$\Gamma(\kappa+1)=\frac{\pi}{\Gamma(-\kappa)\sin(-\kappa\pi)}.$$

Thus, (15) becomes

$$Q(\xi)=\frac{2\pi i}{2^{2\kappa+2}}\frac{\Gamma(2\kappa+2)}{\Gamma(\kappa+1)\Gamma(\kappa+2)}{}_2F_1[1,2\kappa+2;\kappa+2;\tfrac{1}{2}(1-\xi/i\sqrt{\kappa})]. \tag{16}$$

We can now write Z_κ in terms of the hypergeometric function as follows. Upon using Legendre's duplication formula for the Gamma function,[19] i.e.,

$$2^{2z-1}\Gamma(z)\Gamma(z+\tfrac{1}{2})=\pi^{1/2}\Gamma(2z),$$

and substituting (16) into (4) we obtain, finally,

$$Z_\kappa(\xi)=\frac{i(\kappa+\frac{1}{2})(\kappa-\frac{1}{2})}{\kappa^{3/2}(\kappa+1)}\,{}_2F_1[1,2\kappa+2;\kappa+2;\tfrac{1}{2}(1-\xi/i\sqrt{\kappa})]. \tag{17}$$

Equation (17) is valid for all $\kappa>-1$, with the exception of $\kappa=0$, and all ξ, except for those values that lie along the branch cut in $Z_\kappa(\xi)$. By virtue of the branch cut in ${}_2F_1[a,b;c;z]$ extending from 1 to ∞, $Z_\kappa(\xi)$ possesses a branch cut from $-i\sqrt{\kappa}$ to $-i\infty$ along the negative imaginary axis.

At the branch point $\xi=i\sqrt{\kappa}$ of our integrand Z_κ is finite. Using ${}_2F_1[a,b;c;0]=1$, we obtain

$$Z_\kappa(i\sqrt{\kappa})=\frac{i(\kappa+\frac{1}{2})(\kappa-\frac{1}{2})}{\kappa^{3/2}(\kappa+1)}, \tag{18}$$

which agrees with Eq. (18) of Summers and Thorne[16] obtained for integer κ. The latter obtained the above result by evaluation of the residues of their integrand. Result (18) thus serves as a valuable check on the correctness of our formalism and Eq. (17), in particular.

It is perhaps worthwhile commenting, at this point, on our apparent violation of the criterion $\kappa>\frac{3}{2}$ necessary for the convergence of the integral defining the plasma temperature [see the discussion after Eq. (3)]. In the process of deriving a relation for Z_κ in terms of ${}_2F_1[a,b;c;z]$, we have allowed κ to assume even negative values ($\kappa>-1$), and then by the process of analytic continuation we deduce validity for $\kappa>0$. Clearly our definition of plasma temperature breaks down for such negative values as the integral $4\pi\int v^2 f(v)v^2\,dv$ diverges for $\kappa\leqslant\frac{3}{2}$. However, our definition of Z_κ for complex, not necessarily *physical*, argument ξ is independent of the plasma temperature, and as such it does not suffer from the constraint $\kappa>\frac{3}{2}$. In any *physical* problem involving distributions of the form (3), the argument of Z_κ will contain the plasma temperature through the ratio $\xi=\omega/k\theta$, for example, and in this way will be subject to the constraint $\kappa>\frac{3}{2}$.

III. SOME PROPERTIES OF THE FUNCTION Z_κ

The establishment of the connection of Z_κ with Gauss's hypergeometric function is fortunate, in that the theory of the function ${}_2F_1[a,b;c;z]$ is well established and extensive. We may therefore draw freely from it to deduce properties of Z_κ and derive useful relations between the Z_κ, and between Z_κ and other functions. In this section we shall point out some of the more important properties of, and the relations between, the Z_κ; in no way is the list complete. For a more complete listing of some of the more important properties of hypergeometric functions consult Abramowitz and Stegun,[18] for example.

A. Special values of the arguments

Treating the subscript κ as a formal argument, one may deduce from (17) that

$$Z_{1/2}(\xi)\equiv 0, \tag{19}$$

and from the original definition (4) (cf. Summers and Thorne[16]) that

$$Z_\infty(\xi)\equiv Z(\xi), \tag{20}$$

where Z is the plasma dispersion function.[1]

We have already noted in Eq. (18) that

$$Z_\kappa(i\sqrt{\kappa})=\frac{i(\kappa+\frac{1}{2})(\kappa-\frac{1}{2})}{\kappa^{3/2}(\kappa+1)}.$$

It is readily observed, using Gauss' second summation theorem:[20]

$${}_2F_1[a,b;\tfrac{1}{2}(a+b+1);\tfrac{1}{2}]=\frac{\Gamma(\frac{1}{2})\Gamma(\frac{1}{2}+\frac{1}{2}a+\frac{1}{2}b)}{\Gamma(\frac{1}{2}+\frac{1}{2}a)\Gamma(\frac{1}{2}+\frac{1}{2}b)}, \tag{21}$$

and (17) that

$$Z_\kappa(0)=\frac{i\pi^{1/2}}{\kappa^{3/2}}\frac{\Gamma(\kappa+1)}{\Gamma(\kappa-\frac{1}{2})}, \tag{22}$$

which is the generalization to real κ, of Eq. (27) of Summers and Thorne.[16] Using the asymptotic form for the Γ function it is not difficult to show that in the limit $\kappa\to\infty$, Eq. (22) reduces to the familiar result for a Maxwellian plasma, $Z(0)=i\pi^{1/2}$.

B. Differential properties

A differential relation for Z_κ is readily obtained by using the differential properties of the hypergeometric function. The derivative of the hypergeometric function is given by[18,20]

$$\frac{d}{dz}\,{}_2F_1[a,b;c;z]=\frac{ab}{c}\,{}_2F_1[a+1,b+1,c+1;z].$$

Using this relation we, at once, obtain

$$Z'_\kappa(\xi)=-\frac{(\kappa+\frac{1}{2})(\kappa-\frac{1}{2})}{\kappa^2(\kappa+2)}\times{}_2F_1[2,2\kappa+3;\kappa+3;\tfrac{1}{2}(1-\xi/i\sqrt{\kappa})], \tag{23}$$

where the prime denotes differentiation with respect to argument. Using the following relation between contiguous[20] hypergeometric functions,

$$(b-a)\,{}_2F_1[a,b;c;z]+a\,{}_2F_1[a+1,b;c;z]=b\,{}_2F_1[a,b+1;c;z],$$

we can write

$${}_2F_1[2,2\kappa+3;\kappa+3;z]=(2\kappa+3)\,{}_2F_1[2,2\kappa+4;\kappa+3;z]-(2\kappa+2)\,{}_2F_1[1,2\kappa+3;\kappa+3;z] \tag{24}$$

[with $z\equiv\frac{1}{2}(1-\xi/i\sqrt{\kappa})$]. Similarly, using the further relation between contiguous functions,

$$(c-a-b)\,{}_2F_1[a,b;c;z]+b(1-z)\,{}_2F_1[a,b+1;c;z]=(c-a)\,{}_2F_1[a-1,b;c;z],$$

we obtain

$${}_2F_1[2,2\kappa+3;\kappa+3;z]=2(\kappa+2)+i\,\frac{2\kappa+3}{\sqrt{\kappa}}\,\xi\,{}_2F_1[1,2\kappa+4;\kappa+3;z]. \tag{25}$$

Substituting this last Eq. (25) into (23) and noting

$$Z_{\kappa+1}\left[\left(\frac{\kappa+1}{\kappa}\right)^{1/2}\xi\right]=\frac{i(\kappa+\frac{3}{2})}{2(\kappa+1)^{3/2}}\,{}_2F_1[1,2\kappa+4;\kappa+3;\tfrac{1}{2}(1-\xi/i\sqrt{\kappa})],$$

we obtain the desired relation,

$$Z'_\kappa(\xi)=-2\,\frac{(\kappa+\frac{1}{2})(\kappa-\frac{1}{2})}{\kappa^2}\times\left\{1+\frac{\kappa+1}{\kappa+\frac{1}{2}}\left(\frac{\kappa+1}{\kappa}\right)^{1/2}\xi Z_{\kappa+1}\left[\left(\frac{\kappa+1}{\kappa}\right)^{1/2}\xi\right]\right\}, \tag{26}$$

which corresponds to Eq. (34) of Summers and Thorne[16] derived for integer κ. Notice that as $\kappa\to\infty$, Eq. (26) reduces to the usual relation between the derivative of the Z function of Fried and Conte[1] and the function itself (cf. Ref. 16), i.e.,

$$Z'(\xi)=-2[1+\xi Z(\xi)],$$

as is to be expected.

C. Symmetry property

Comparing Eq. (A7) from the Appendix with Eq. (17) we deduce the following symmetry relation for Z_κ:

$$Z_\kappa(\xi)=\frac{2i\pi^{1/2}\Gamma(\kappa+1)}{\kappa^{3/2}\Gamma(\kappa-\frac{1}{2})}\left(1+\frac{\xi^2}{\kappa}\right)^{-(\kappa+1)}-Z_\kappa(-\xi). \tag{27}$$

D. Integer κ: correspondence with Z_κ^*

The correspondence of the function Z_κ for integral κ, with the function[16] Z_κ^* is readily demonstrated using the definition of the hypergeometric series,

$${}_2F_1[a,b;c;z]=\sum_{n=0}^{\infty}\frac{(a)_n(b)_n}{(c)_n}\frac{z^n}{n!};\quad |z|<1. \tag{28}$$

The notation $(a)_n$ denotes $a(a+1)(a+2)\cdots(a+n-1)=\Gamma(a+n)/\Gamma(a)$ (see, e.g., Abramowitz and Stegun;[18] and Slater[20]). With the definition (28) one has, by (17),

$$Z_\kappa(\xi)=\frac{i(\kappa-\frac{1}{2})}{2\kappa^{3/2}}\frac{\Gamma(\kappa+1)}{\Gamma(2\kappa+1)}\sum_{n=0}^{\infty}\frac{\Gamma(2\kappa+2+n)}{\Gamma(\kappa+2+n)}\times\left[\frac{1}{2}\left(1-\frac{\xi}{i\sqrt{\kappa}}\right)\right]^n,$$

for $|\xi-i\sqrt{\kappa}|<2\sqrt{\kappa}$.

Now if κ is integral, i.e., $\kappa=k$, then one can relabel the summation indices to read as

$$Z_k(\xi)=\frac{i(k-\frac{1}{2})}{2k^{3/2}}\frac{k!}{(2k)!}\sum_{l=k+1}^{\infty}\frac{(k+l)!}{l!}\times\left[\frac{1}{2}\left(1-\frac{\xi}{i\sqrt{k}}\right)\right]^{l-k-1}.$$

Then, splitting the sum into the difference of $\Sigma_{l=0}^{\infty}$ and $\Sigma_{l=0}^{k}$, and manipulating, one obtains

$$Z_k(\xi)=\frac{2\pi^{1/2}i}{(1+\xi^2/k)^{k+1}}\frac{k!}{k^{3/2}\Gamma(k-\frac{1}{2})}\times\left(1-\frac{(1+\xi/i\sqrt{k})^{k+1}}{k!\,2^{k+1}}\times\sum_{l=0}^{k}\frac{(k+l)!}{l!}\frac{(1-\xi/i\sqrt{k})^l}{2^l}\right), \tag{29}$$

which is identical (for $\kappa=k$) to Eq. (17) of Summers and Thorne,[16] defining their function $Z_\kappa^*(\xi)$ for integer κ. Note that while we assumed *ab initio* that $|\xi-i\sqrt{k}|<2\sqrt{k}$ our result (29) is in fact the analytic continuation into the entire complex plane because the series terminates.

In a similar manner, using (A6) (from the Appendix) in (4) one can show that for integer $\kappa=k$ we obtain the reduced form for Z_κ^*, of Summers and Thorne[16] [their Eq. (20)]:

$$Z_k(\xi)=-\frac{(k-\frac{1}{2})}{2k^{3/2}}\frac{k!}{(2k)!}\sum_{l=0}^{k}\frac{(k+l)!}{l!}\,i^{k-l}\left(\frac{2}{\xi/\sqrt{k}+i}\right)^{k+1-l}. \tag{30}$$

Furthermore, beginning with (A8) from the Appendix, one could, of course, obtain a rational polynomial expression for $Z_k(\xi)$ in terms of $(1-\xi/i\sqrt{k})$ and $(1+\xi/i\sqrt{k})$.

E. Taylor series: $|\xi|\ll 1$

Perhaps the simplest and most direct way to obtain a Taylor series expansion about the point $\xi=0$ for Z_κ is to employ the definition of the Taylor series in conjunction with the formula[18]

$$\frac{d^n}{dz^n}\,{}_2F_1[a,b;c;z]=\frac{(a)_n(b)_n}{(c)_n}\,{}_2F_1[a+n,b+n;c+n;z].$$

Using these with Gauss' second summation theorem (21) and the duplication formula for the Gamma function, one can derive the following Taylor expansion for Z_κ, starting with the definition (17):

$$Z_\kappa(\xi)=\frac{i\pi^{1/2}}{\kappa^{3/2}\Gamma(\kappa-\frac{1}{2})}\sum_{n=0}^{\infty}\left(\frac{-1}{i\sqrt{\kappa}}\right)^n\frac{\Gamma[\kappa+\frac{1}{2}(n+2)]}{\Gamma[\frac{1}{2}(n+2)]}\,\xi^n. \tag{31}$$

Equation (31) can be recast in a form analogous to the usual Taylor expansion of the Z function by separating the series into odd and even term series:

$$Z_\kappa(\xi)=\frac{i\pi^{1/2}\Gamma(\kappa+1)}{\kappa^{3/2}\Gamma(\kappa-\frac{1}{2})}\left(1+\frac{\xi^2}{\kappa}\right)^{-(\kappa+1)}-\frac{\pi^{1/2}}{\kappa^2\Gamma(\kappa-\frac{1}{2})}\,\xi\sum_{n=0}^{\infty}\frac{(-1)^n}{\kappa^n}\frac{\Gamma(\kappa+n+\frac{3}{2})}{\Gamma(n+\frac{3}{2})}\,\xi^{2n}. \tag{32}$$

As is readily checked, both series representations have a radius of convergence of $|\xi|<\sqrt{\kappa}$.

In the form (32) the series bears considerable similarity to the power series expansion of the Z function, where it is usual to separate out the exponential term [the analogous term here is the one containing $(1+\xi^2/\kappa)^{-(\kappa+1)}$] from the rest of the series. The advantage of the series in this form is that the approximations usually associated with the exponential term in the power series of the Z function are easily transferred to the term containing $(1+\xi^2/\kappa)^{-(\kappa+1)}$ for Z_κ. Furthermore, these series, (31) and (32), are precisely those derived by Summers and Thorne[16] [see their Eqs. (27) and (28)] for integer κ, using an alternative method. This is readily verified by writing out the first few terms.

As a byproduct of the above analysis we obtain a further formula relating Z_κ to the hypergeometric function. Writing the Γ functions in the sum in (32) in terms of the Pochhammer symbols $(a)_n$, we deduce the following relation [using Eq. (28)]:

$$Z_\kappa(\xi)=\frac{i\pi^{1/2}\Gamma(\kappa+1)}{\kappa^{3/2}\Gamma(\kappa-\frac{1}{2})}\left(1+\frac{\xi^2}{\kappa}\right)^{-(\kappa+1)}-\frac{2i(\kappa+\frac{1}{2})(\kappa-\frac{1}{2})}{\kappa^{3/2}}\frac{\xi}{i\sqrt{\kappa}}\,{}_2F_1\left[1,\kappa+\frac{3}{2};\frac{3}{2};\frac{-\xi^2}{\kappa}\right].$$

F. Taylor series: $|\xi^{-1}|\ll 1$

To obtain a Taylor series for $|1/\xi|\ll 1$, we employ the relation[18]

$$\begin{aligned}{}_2F_1[a,b;c;z]=&\frac{\Gamma(c)\Gamma(b-a)}{\Gamma(b)\Gamma(c-a)}(-z)^{-a}\times{}_2F_1\left[a,1+a-c;1+a-b;\frac{1}{z}\right]\\&+\frac{\Gamma(c)\Gamma(a-b)}{\Gamma(a)\Gamma(c-b)}(-z)^{-b}\times{}_2F_1\left[b,1+b-c;1+b-a;\frac{1}{z}\right],\end{aligned}$$

such that $|\arg(-z)|<\pi$. This enables us to write

$$\begin{aligned}&{}_2F_1[1,2\kappa+2;\kappa+2;\tfrac{1}{2}(1-\xi/i\sqrt{\kappa})]\\&=-\frac{(\kappa+1)}{(2\kappa+1)}\frac{2}{(1-\xi/i\sqrt{\kappa})}\times{}_2F_1\left[1,-\kappa;-2\kappa;2\Big/\left(1-\frac{\xi}{i\sqrt{\kappa}}\right)\right]\\&\quad-\frac{\pi^{1/2}\Gamma(\kappa+2)}{\cos(\pi\kappa)\Gamma(\kappa+\frac{3}{2})}\left(\frac{\xi}{i\sqrt{\kappa}}-1\right)^{-(\kappa+1)}\times\left(\frac{\xi}{i\sqrt{\kappa}}+1\right)^{-(\kappa+1)},\end{aligned} \tag{33}$$

(for $|\arg(\xi/i\sqrt{\kappa}-1)|<\pi$) where we have used, among others, the fact that ${}_2F_1[2\kappa+2,\kappa+1;2\kappa+2;z]={}_2F_1[\kappa+1,2\kappa+2;2\kappa+2;z]=(1-z)^{-(\kappa+1)}$. Using the definition of the hypergeometric series (28) and the binomial theorem, we can readily express the first term on the right-hand side of (33) as the double series,

$$\begin{aligned}&=\frac{(\kappa+1)}{\kappa+\frac{1}{2}}\frac{i\sqrt{\kappa}}{\xi}\sum_{n=0}^{\infty}\sum_{p=n}^{\infty}(-1)^n2^n(i\sqrt{\kappa})^p\times\frac{(-\kappa)_n(n+1)_{p-n}}{(-2\kappa)_n(p-n)!}\left(\frac{1}{\xi}\right)^p,\\&=\frac{(\kappa+1)}{\kappa+\frac{1}{2}}\frac{i\sqrt{\kappa}}{\xi}\sum_{p=0}^{\infty}(i\sqrt{\kappa})^p\left(\frac{1}{\xi}\right)^p\times\sum_{n=0}^{p}(-1)^n2^n\frac{(-\kappa)_n(n+1)_{p-n}}{(-2\kappa)_n(p-n)!}.\end{aligned}$$

With a little manipulation, the coefficient of $1/\xi^p$ can be shown to be

$$=(i\sqrt{\kappa})^p \sum_{n=0}^{p} \frac{(-p)_n(-\kappa)_n}{(-2\kappa)_n} \frac{2^n}{n!};$$

$$=(i\sqrt{\kappa})^p {}_2F_1[-p,-\kappa;-2\kappa;2], \tag{34}$$

where we have used the relations

$$(1+n)_{p-n}=\frac{(1)_p}{(1)_n}; \quad \frac{1}{(p-n)!}=\frac{(-p)_n(-1)^n}{p!}.$$

To evaluate ${}_2F_1[-p,-\kappa;-2\kappa;2]$ we first apply the quadratic transformation formula,[18]

$$_2F_1[a,b;2b;z]$$
$$=(1-z)^{-a/2} {}_2F_1[\tfrac{1}{2}a,b-\tfrac{1}{2}a;b+\tfrac{1}{2};z^2/(4z-4)],$$

to yield $i^p {}_2F_1[-\frac{1}{2}p,-\kappa+\frac{1}{2}p;-\kappa+\frac{1}{2};1]$. This is easily evaluated by Gauss' summation theorem:

$$_2F_1[a,b;c;1]=\frac{\Gamma(c)\Gamma(c-a-b)}{\Gamma(c-a)\Gamma(c-b)}, \quad \mathrm{Re}(c-a-b)>0,$$

yielding

$$i^p \pi^{1/2} \frac{\Gamma(-\kappa+\frac{1}{2})}{\Gamma[-\kappa+\frac{1}{2}(1+p)]\Gamma[\frac{1}{2}(1-p)]}. \tag{35}$$

Now, note that the term $\Gamma[\frac{1}{2}(1-p)]$ in the denominator of (35) will cause odd powers of $1/\xi$ to be zero. Thus, relabeling, substituting the series back into (33), and, in turn, substituting this expression into (17) yields the required series expansion:

$$Z_\kappa(\xi)=-\frac{i\pi^{1/2}\Gamma(\kappa+1)}{\kappa^{3/2}\cos(\pi\kappa)\Gamma(\kappa-\frac{1}{2})}\left(\frac{\xi}{i\sqrt{\kappa}}-1\right)^{-(\kappa+1)}$$
$$\times\left(\frac{\xi}{i\sqrt{\kappa}}+1\right)^{-(\kappa+1)}-\frac{(2\kappa-1)}{2\kappa}\frac{1}{\xi}\sum_{n=0}^{\infty}\kappa^n$$
$$\times\frac{\pi^{1/2}}{\Gamma(-n+\frac{1}{2})}\frac{\Gamma(-\kappa+\frac{1}{2})}{\Gamma(-\kappa+\frac{1}{2}+n)}\xi^{-2n}. \tag{36}$$

Note that for real κ we cannot, in general, write $(\xi/i\sqrt{\kappa}-1)^{-(\kappa+1)}(\xi/i\sqrt{\kappa}+1)^{-(\kappa+1)}=(-\xi^2/\kappa-1)^{-(\kappa+1)}$.

For integer κ the series (36) reduces to that found by Summers and Thorne[16] [their Eq. (30)], which can be seen by writing out the first few terms. Furthermore, note that the series is *divergent* for half-integer κ.

G. Integral representations

In addition to the definition, which is analogous to that used by Summers and Thorne:[16]

$$Z_\kappa(\xi)=\frac{1}{\pi^{1/2}\kappa^{3/2}}\frac{\Gamma(\kappa+1)}{\Gamma(\kappa-\frac{1}{2})}\int_L\frac{ds}{(s-\xi)(1+s^2/\kappa)^{\kappa+1}}, \tag{37}$$

where the Landau contour L goes from $-\infty$ to ∞, passing below the pole $s=\xi$, we have derived the alternative Pochhammer-like integral representation,

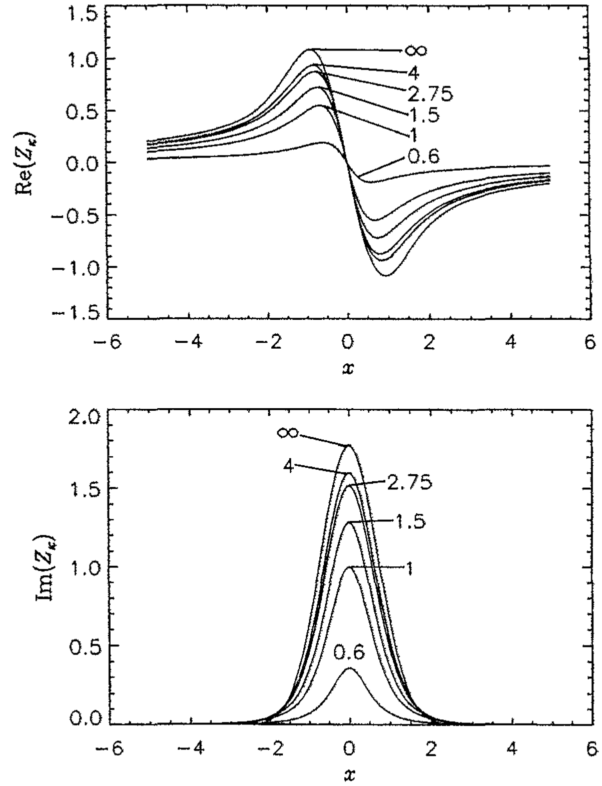

FIG. 2. *Top panel*: the real and, *bottom panel*: imaginary parts of $Z_\kappa(x)$ for real x. Parameter labeling curves is κ.

$$Z_\kappa(\xi)=\frac{\Gamma(\kappa+1)}{2^{2\kappa+2}\pi^{1/2}\kappa^{3/2}}\int_C t^{2\kappa+1}(t-1)^{-(\kappa+1)}$$
$$\times\left[1-t\left(\frac{i\sqrt{\kappa}-\xi}{2i\sqrt{\kappa}}\right)\right]^{-1}dt, \tag{38}$$

where the contour C is a loop beginning at $0-0i$, encircling the branch point $t=1$ in an anticlockwise direction, and terminating at $0+0i$.

IV. GEOMETRICAL FEATURES OF Z_κ

In this section we present some numerical results and discuss the geometrical properties and topology of the function Z_κ for a few values of κ. Summers and Thorne[16] have discussed, comprehensively, the topology of the function Z_κ^* and its similarities to that of the Z function,[1] and many of their comments are applicable to the more general function Z_κ. We shall concentrate here on nonintegral values of κ.

Figure 2 illustrates the real and imaginary parts of $Z_\kappa(x)$ for real x, i.e., we consider only those values of Z_κ along the real line. We observe a trend similar to that found by Summers and Thorne,[16] namely that the ranges spanned by the real and imaginary parts of Z_κ exhibit monotonic increases as κ is increased. Note, however, that with our definition $\kappa<1$ is allowed with $Z_{1/2}=0$, identically. While such small values of κ are of academic interest they are unlikely to find much practical application. Note further, that the curves for $\kappa=1$ are exactly the same as those illustrated previously by

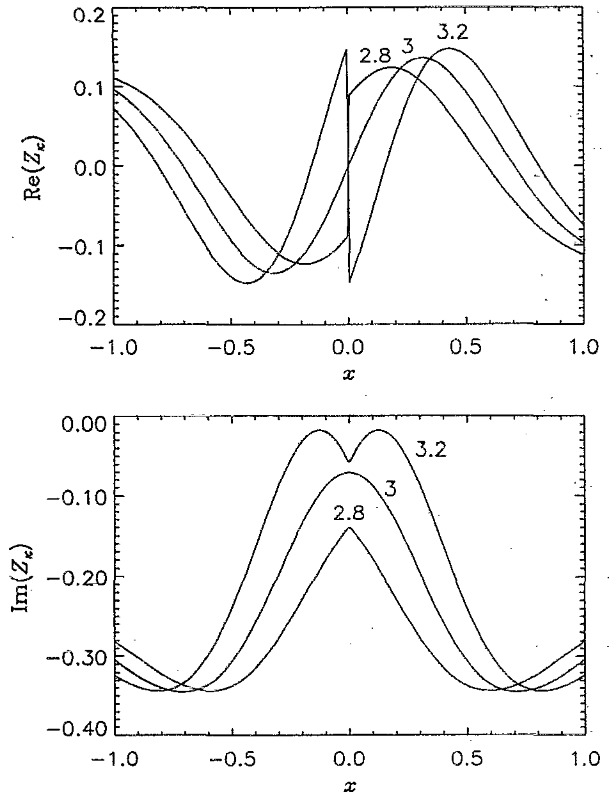

FIG. 3. *Top panel*: the real and, *bottom panel*: imaginary parts of $Z_\kappa(x-3i)$ in the neighborhood of their branch cuts. Parameter labeling curves is κ.

Summers and Thorne[16] (their Fig. 4), as the analyses of the previous sections predict. The curve labeled $\kappa=\infty$ represents the Fried and Conte Z function.

Perhaps the biggest difference between Z_κ and Z_κ^* is the presence of a branch point, $\xi=-i\sqrt{\kappa}$ in the former. The branch line extends from $-i\infty$ to $-i\sqrt{\kappa}$ along the negative imaginary axis. It should be mentioned, however, that Z_κ^* is discontinuous at the point $\xi=-i\sqrt{\kappa}$ also. The discontinuity in that case results due to the nonexistence of the limit[16] as $\xi\equiv x+iy\rightarrow-i\sqrt{\kappa}$. Figure 3 illustrates the behavior of $Z_\kappa(x-3i)$, for a few values of κ, in a neighborhood, $y=-3<-\sqrt{\kappa}$, of the branch point $-i\sqrt{\kappa}$. Note that there is no branch cut for $\kappa=3$, and both the curves representing the real and imaginary parts, respectively, are continuous and differentiable at $x=0$. However, the curves for $\kappa=2.8$ and 3.2 exhibit otherwise: neither the real nor the imaginary part of $Z_\kappa(x-3i)$ is differentiable at $x=0$, and furthermore, the real parts are discontinuous. One also observes the oscillatory nature of the function in the vicinity of $\xi=-i\sqrt{\kappa}$, and this structure is enhanced as one more closely approaches the branch point $-i\sqrt{\kappa}$.

Figure 4 illustrates the behavior of the function $Z_{2.4}(\xi)$ as a function of $\xi=x+iy$. In (a) and (b) the surfaces representing the real and imaginary parts of $Z_{2.4}(\xi)$ are illustrated, while (c) and (d) illustrate contour levels of the real and imaginary parts, respectively. In (c) and (d) the lighter

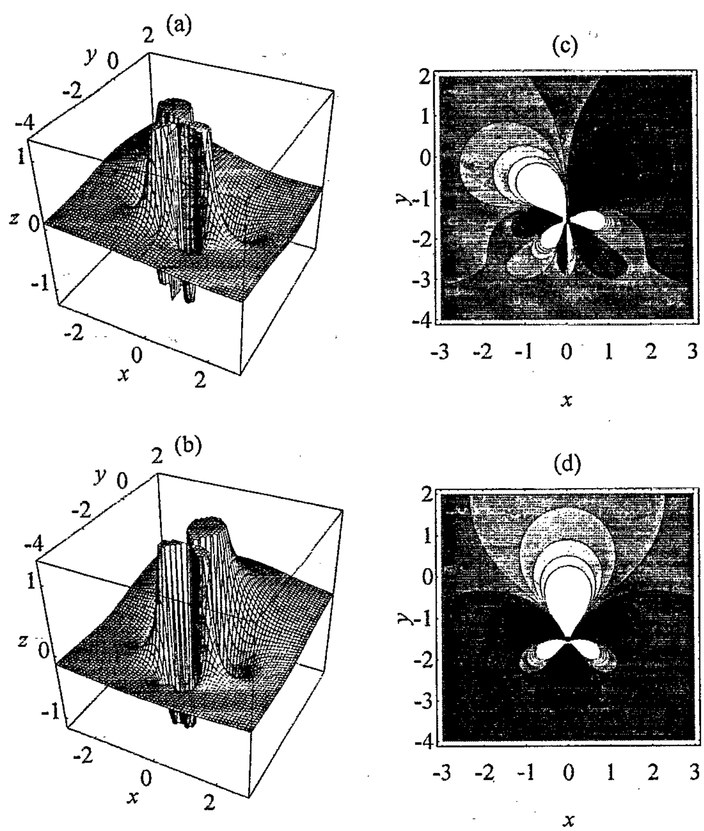

FIG. 4. Surfaces denoting the real (a) and imaginary (b) parts, and contours denoting the real (c) and imaginary (d) parts, of $Z_{2.4}(\xi)$.

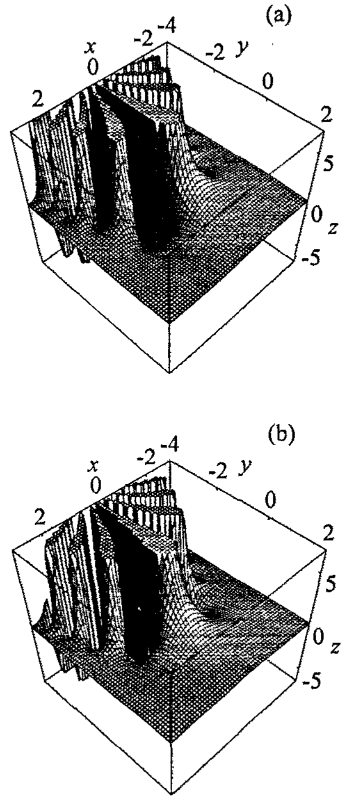

FIG. 5. Surfaces denoting the real (a) and imaginary (b) parts of $Z_{26.6}(\xi)$.

shades represent higher points, while the darker shades represent the lower. Note the obvious discontinuity marking the branch line in (a). Furthermore, note the approximately $\kappa+1$ dark and $\kappa+1$ light lobes in (c) and (d).

In Fig. 5 we illustrate the real (a) and imaginary (b) surfaces of Z_κ for the relatively large value of $\kappa=24.6$. At these large values of κ the real and imaginary surfaces of the function Z_κ are qualitatively very similar to those of the Z function.[1] We have changed the viewpoint from our earlier plot (Fig. 4) and we are now looking from a vantage point corresponding to positive x, y, and z. Note the many "ridge" or "buttress" structures of the real and imaginary surfaces viewed from this angle. Such behavior is strikingly similar to that of the Fried and Conte Z function.[1] Note that as κ is increased the branch point at $\xi=-i\sqrt{\kappa}$ will have less of an effect on the topology of the function for values of ξ with moderate, negative imaginary parts. This means that normal mode wave behavior [where normal mode refers to those waves that suffer only weak damping, i.e., they have small $-\gamma$ and consequently small $|\mathrm{Im}\,(\xi)|$] can be expected to approach that expected for a plasma in which the particle distributions are Maxwellian. Moreover, note that as $\kappa\to\infty$, Z_κ becomes an entire function as the branch point recedes to $-i\infty$. This is a necessary requirement for the coincidence of Z_∞ with Z.

In summary, the functions Z_κ and Z_κ^* exhibit very similar behavior over the entire complex plane, with the exception of the negative imaginary axis. As pointed out previously, Z_κ possesses a branch point on this axis at $-i\sqrt{\kappa}$ and a branch line that extends from this point to $-i\infty$. Interestingly though, Z_κ^* exhibits discontinuous behavior at the point $-i\sqrt{\kappa}$ as well.[16] The similarity in the behavior of the two functions (Z_κ^* is, as we have shown, a special case of Z_κ) makes it possible, given dispersion relations calculated for integer values of κ, i.e., using Z_κ^*, to deduce, crudely, the behavior for nonintegral values of κ by interpolation. However, care must be exercised when the complex solution representing the wave mode lies near the negative imaginary axis. On the other hand, such waves modes are physically not very interesting.

V. APPLICATION: ELECTROSTATIC WAVES IN A NONTHERMAL PLASMA

We have chosen the example of Langmuir or electron plasma waves in an unmagnetized plasma for illustrative purposes; the treatment is not complete and only serves to demonstrate the use of Z_κ. Thorne and Summers[10] have comprehensively investigated Langmuir waves in a plasma composed of kappa distributions for the cases $\kappa=2$ and $\kappa=3$. Here we concentrate on nonintegral values of κ.

Employing the equation for the dielectric function for electrostatic waves in an unmagnetized plasma,[21]

$$\epsilon(\mathbf{k},\omega)=1+\sum_j \frac{\omega_{pj}^2}{k^2}\int \frac{\mathbf{k}\cdot\nabla f_j^{(0)}}{\omega-\mathbf{k}\cdot\mathbf{v}}\,d^3\mathbf{v} \tag{39}$$

(where $\omega\equiv\omega_r+i\gamma$ is the complex wave frequency) and substituting kappa distributions for the $f_j^{(0)}$'s, we readily obtain (see Refs. 16, 10 and Appendix A of Ref. 11, for example)

$$\epsilon(\mathbf{k},\omega)=1+2\sum_j \frac{\omega_{pj}^2}{k^2\theta_j^2}\left[\frac{2\kappa_j-1}{2\kappa_j}+\frac{\omega}{k\theta_j}Z_{\kappa_j}\left(\frac{\omega}{k\theta_j}\right)\right]. \tag{40}$$

The solutions to $\epsilon(\mathbf{k},\omega)=0$ define the electrostatic modes of the plasma. Note that we have allowed each plasma species j to possess its own κ_j for generality. On the grounds of shock acceleration theory or stochastic acceleration by plasma waves different κ_j are a distinct possibility if the plasma components have widely disparate masses (such as electrons and protons, for example).

We seek an electrostatic wave, whose phase speed satisfies

$$\left|\frac{\omega}{k\theta_i}\right|\gg\left|\frac{\omega}{k\theta_e}\right|\gg 1,\quad \text{or}\quad |\xi_i|\gg|\xi_e|\gg 1.$$

This ordering enables us to expand asymptotically [using (36)] the Z_κ functions in (40) as follows:

$$Z_{\kappa_i}(\xi_i)\simeq-\frac{(2\kappa_i-1)}{2\kappa_i}\frac{1}{\xi_i}; \tag{41}$$

$$Z_{\kappa_e}(\xi y_e)\simeq-\frac{i\pi^{1/2}\Gamma(\kappa_e+1)}{\kappa_e^{3/2}\cos(\kappa_e\pi)\Gamma(\kappa_e-\frac{1}{2})}\left(\frac{i\sqrt{\kappa_e}}{\xi_e}\right)^{2\kappa_e+2} -\frac{(2\kappa_e-1)}{2\kappa_e}\frac{1}{\xi_e}-\frac{1}{2}\frac{1}{\xi_e^3}-\frac{3}{2}\frac{\kappa_e}{(2\kappa_e-3)}\frac{1}{\xi_e^5}. \tag{42}$$

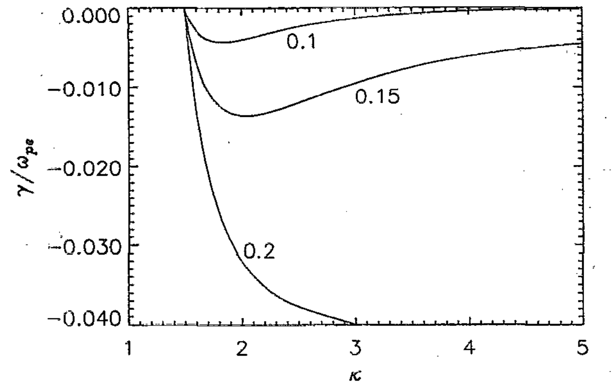

FIG. 6. Damping rate (45) as a function of $\kappa \equiv \kappa_e$ for the Langmuir wave. The parameter labeling the curves is the wave number, $k\lambda_{De}$.

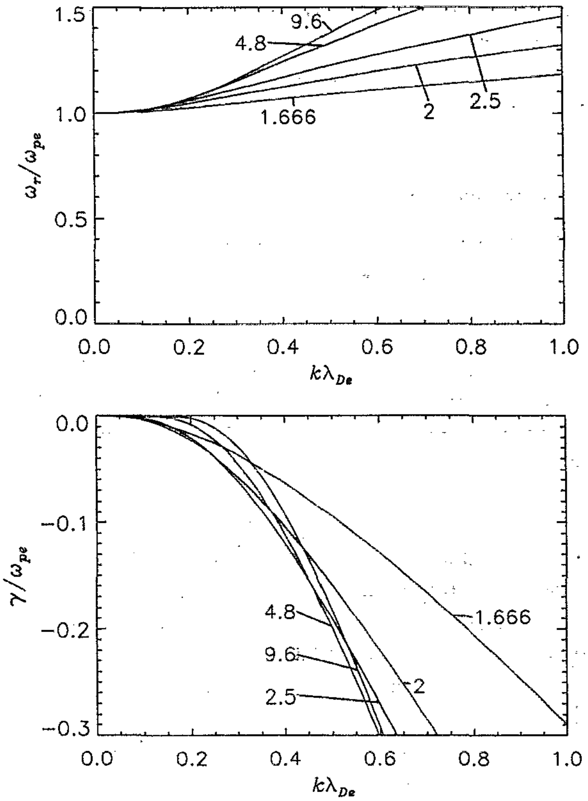

FIG. 7. Dispersion relation (*top panel*) and damping rate (*bottom panel*) for Langmuir waves in a nonthermal plasma of electrons and ions. Parameter labeling the curves is κ_e, the spectral index of the electron distribution.

In this approximation, (40) becomes

$$1+2\,\frac{\omega_{pe}^2}{k^2\theta_e^2}\left[\frac{\pi^{1/2}\Gamma(\kappa_e+1)}{\kappa_e\cos(\kappa_e\pi)\Gamma(\kappa_e-\frac{1}{2})}\left(i\sqrt{\kappa_e}\,\frac{k\theta_e}{\omega}\right)^{2\kappa_e+1}-\frac{1}{2}\,\frac{k^2\theta_e^2}{\omega^2}-\frac{3}{2}\,\frac{\kappa_e}{(2\kappa_e-3)}\,\frac{k^4\theta_e^4}{\omega^4}\right]=0. \tag{43}$$

Assuming $|\gamma|\ll|\omega_r|$, the real part of (43) yields

$$\omega_r^2=\omega_{pe}^2+3\,\frac{\kappa_e}{2\kappa_e-3}\,k^2\theta_e^2=\omega_{pe}^2+3k^2v_e^2, \tag{44}$$

because $\theta_e\equiv[(2\kappa_e-3)/\kappa_e]^{1/2}v_e$—where v_e is the electron thermal velocity, $(T_e/m_e)^{1/2}$. Thus, the dispersion relation for Langmuir waves in a plasma composed of κ-distributed electrons is identical, for small $|k|$, to that for a plasma in which the electron distribution is a Maxwellian.

The damping rate, however, is significantly different, as has been pointed out previously.[10] The imaginary part of (43) yields

$$\gamma=-\pi^{1/2}\,\frac{\Gamma(\kappa_e+1)}{\Gamma(\kappa_e-\frac{1}{2})}\,\kappa_e^{\kappa_e-1/2}k\theta_e\left(\frac{k^2\theta_e^2}{\omega_r^2}\right)^{\kappa_e-1}$$
$$\simeq-\pi^{1/2}\,\frac{\Gamma(\kappa_e+1)}{\Gamma(\kappa_e-\frac{1}{2})}\,\omega_{pe}(2\kappa_e-3)^{\kappa_e-1/2}(k^2\lambda_{De}^2)^{\kappa_e-1/2}, \tag{45}$$

where $\lambda_{De}\equiv(T_e/4\pi n_e e^2)^{1/2}$ is the electron Debye screening length. A similar expression for the damping rate was derived initially by Thorne and Summers,[10] assuming integer values of κ_e and, as we have demonstrated here, is equally valid for real $\kappa_e>\frac{3}{2}$. As pointed out by Thorne and Summers,[10] the damping rate of Langmuir waves in a plasma of kappa-distributed electrons is *strongly* dependent on κ_e—the spectral index of the electron distribution. However, since our expressions are valid for real κ_e we can more finely probe this behavior, and we are not limited to a discrete set of points. It is found that for sufficiently small values of $k\lambda_{De}$, the damping rate exhibits a monotonic decrease in magnitude with κ_e for larger κ_e. This is observed in the curve for $k\lambda_{De}=0.1$ in the region $\kappa_e>2$ in Fig. 6, obtained using (45). However, above a certain wave number the damping rate *increases* monotonically for increasing values of κ_e as seen from the curve for $k\lambda_{De}=0.2$. It should be noted that with the approximations used to obtain (45) the region $\kappa_e<2$ in Fig. 6 is, at best, qualitative (see the next paragraph).

There are a number of points worthy of mention. In deriving the wave frequency/dispersion relation and growth rate, we have tacitly assumed that $2\kappa_e+2$ is significantly larger than 5—the order to which we have carried out our asymptotic expansion in ξ^{-1}. Were this not the case, we would have had to include a term proportional to

$$\tan(\kappa_e\pi)\left(\frac{k\theta_e}{\omega_r}\right)^{2\kappa_e+1},$$

in the real part of the dispersion relation, making an algebraic solution for ω, in general, impossible. Furthermore, numerical solution of the exact electrostatic dispersion relation (40) (see Fig. 7) indicates that the real part of the frequency is quite strongly dependent on κ_e, even for relatively small values of $k\lambda_{De}\sim0.25$. This should be contrasted with the behavior predicted by our approximate analysis (44), which shows that ω_r is independent of κ_e. This difference implies that terms higher than ξ^{-5} in the expansion of $Z_{\kappa_e}(\xi_e)$ are important in defining the behavior of Langmuir waves at moderate wave numbers and a numerical solution might be called for. Figure 7 shows that the approximate analytic approach is only accurate for $k\lambda_{De}\leqslant0.1$, especially for small values of κ_e.

Figure 7 also clearly exhibits the decrease in the damping of Langmuir waves at small wave number, for increasing κ_e. Again, for $0.1<k\lambda_{De}<0.3$ there is significant variation of growth rate with κ_e for $\kappa_e<4.8$.

VI. CONCLUSIONS

We have introduced a new special function denoted by $Z_\kappa(\xi)$, which arises in kinetic studies of waves in space plasmas in which one or more particle distributions are modeled by kappa distributions. The function $Z_\kappa(\xi)$, valid for all real positive κ—the parameter that shapes the superthermal particle tail—is a generalization of the function Z_κ^*, valid only for integer values of κ, introduced by Summers and Thorne.[16]

For real values of κ one loses the advantages of being able to write Z_κ as a rational polynomial on the one hand, but on the other one gains, as we have demonstrated, the close relation to the important and very well-known Gauss hypergeometric function, ${}_2F_1[1,2\kappa+2;\kappa+2;z]$. This close relationship enables one to manipulate and simplify dispersion relations using the well-established and extensive theory of ${}_2F_1[a,b;c;z]$, and, furthermore, for analytical purposes where power series and asymptotic forms are often called for, the order of complexity is comparable whether one uses the Z_κ or Z_κ^* of Summers and Thorne.[16]

The existence of a broader mathematical foundation enables one to use the simpler Z_κ^* through interpolation to obtain *qualitative* results for noninteger κ, and justifies such a step.

Since it is now well established on the basis of theory and observation that space and astrophysical plasmas often contain supra- and superthermal particles and that the kappa distribution offers a useful fit to their "spectral" distribution we expect that the function Z_κ should be a useful tool in advancing the kinetic theory of waves in space plasmas—especially in the vicinity of shock waves and sites where nonthermal processes efficiently accelerate particles to superthermal energies. Previous works on plasmas containing generalized Lorentzian particle distributions with integer values of κ have already begun to indicate significant differences from their Maxwellian plasma analogs, especially in terms of wave damping by the overabundance of particles with velocities in excess of the thermal speed.

It should be stressed that while we have used the isotropic form of the kappa distribution for simplicity, other anisotropic forms analogous to the bi-Maxwellian and loss-cone distributions can be constructed (see Table I of Ref. 16, for example) and may be useful in modeling magnetized plasmas. If, for example, the distribution of velocities parallel to the magnetic field can be described by the functional form $\propto(1+v_\parallel^2/\kappa\theta_\parallel^2)^{-(\kappa+1)}$—such as in the product bi-Lorentzian,[16,22]

$$f(v_\perp,v_\parallel)=\pi^{-3/2}(\theta_\perp^2\theta_\parallel\kappa^{1/2})^{-1}\frac{\Gamma(\kappa+1)}{\Gamma(\kappa+\frac{1}{2})}\times\left(1+\frac{v_\perp^2}{\kappa\theta_\perp^2}\right)^{-(\kappa+1)}\left(1+\frac{v_\parallel^2}{\kappa\theta_\parallel^2}\right)^{-(\kappa+1)},$$

then the dispersion function Z_κ will play an important role.

In conclusion, we comment briefly on the numerical evaluation of Z_κ. All the numerical calculations performed in this paper have been done using the software package MATHEMATICA, employing the internal function Hypergeometric2F1 defined therein. Press *et al.*[23] describe an efficient method of evaluating numerically the hypergeometric function for arbitrary values of its arguments and present an algorithm for its evaluation.

APPENDIX: ALTERNATIVE CONTOUR OF INTEGRATION

In this appendix we demonstrate an alternative integration contour [see Fig. 1(c)] for the evaluation of Z_κ in terms of the hypergeometric function. We close the contour of integration upward and loop anticlockwise about the branch point $s=i\sqrt{\kappa}$. The integrals along the semicircular segments vanish as before. We can then write

$$\oint_C \frac{ds}{(s-\xi)(1+s^2/\kappa)^{\kappa+1}}=Q(\xi)+\int_B\frac{ds}{(s-\xi)(1+s^2/\kappa)^{\kappa+1}}=2\pi i\ \mathrm{Res}(\xi),\quad \text{(A1)}$$

where in the last step we have used the residue theorem.

Applying the transformation

$$t=\frac{2}{1+s/i\sqrt{\kappa}},\quad \text{(A2)}$$

to the integral around the branch, I_B, yields

$$I_B=\frac{-1}{2^{2\kappa+2}}\int_{B'}t^{2\kappa+1}(t-1)^{-(\kappa+1)}\times\left[1-t\left(\frac{\xi+i\sqrt{\kappa}}{2i\sqrt{\kappa}}\right)\right]^{-1}dt,\quad \text{(A3)}$$

where the subscript B' on the integral denotes the new contour [under the transformation (A2)]. Integrating around the branch in the t plane as before, and making the connection with the hypergeometric function, we obtain

$$I_B=i\pi^{1/2}\frac{\Gamma(\kappa+\frac{3}{2})}{\Gamma(\kappa+2)}\,{}_2F_1[1,2\kappa+2;\kappa+2;\tfrac{1}{2}(1+\xi/i\sqrt{\kappa})],\quad \text{(A4)}$$

valid for all real κ except integer $\kappa<-1$, as before.

We can now write Z_κ in terms of the hypergeometric function as follows. The residue, $\mathrm{Res}(\xi)$ is readily evaluated:[16]

$$\mathrm{Res}(\xi)=(1+\xi^2/\kappa)^{-(\kappa+1)}.\quad \text{(A5)}$$

Substituting this and (A4) into (A1) yields

$$Q(\xi)=\frac{2\pi i}{(1+\xi^2/\kappa)^{\kappa+1}}-i\pi^{1/2}\frac{\Gamma(\kappa+\frac{3}{2})}{\Gamma(\kappa+2)}\times{}_2F_1\left[1,2\kappa+2;\kappa+2;\frac{1}{2}\left(1+\frac{\xi}{i\sqrt{\kappa}}\right)\right],\quad \text{(A6)}$$

thus

$$Z_\kappa(\xi)=\frac{2i\pi^{1/2}\Gamma(\kappa+1)}{\kappa^{3/2}\Gamma(\kappa-\frac{1}{2})}\left(1+\frac{\xi^2}{\kappa}\right)^{-(\kappa+1)} - \frac{i(\kappa+\frac{1}{2})(\kappa-\frac{1}{2})}{\kappa^{3/2}(\kappa+1)} \times {}_2F_1\left[1,2\kappa+2;\kappa+2;\frac{1}{2}\left(1+\frac{\xi}{i\sqrt{\kappa}}\right)\right]. \quad \text{(A7)}$$

Further simplification results using the relation[18]

$$ {}_2F_1[a,b;c;z]=\frac{\Gamma(c)\Gamma(c-a-b)}{\Gamma(c-a)\Gamma(c-b)}\, z^{-a}{}_2F_1[a,a-c+1;a+b-c+1;1-1/z] + \frac{\Gamma(c)\Gamma(a+b-c)}{\Gamma(a)\Gamma(b)}\,(1-z)^{c-a-b}z^{a-c} \times {}_2F_1[c-a,1-a;c-a-b+1;1-1/z],$$

($|\arg(z)|<\pi$, $|\arg(1-z)|<\pi$), yielding

$$Z_\kappa(\xi)=\frac{2i(\kappa+\frac{1}{2})(\kappa-\frac{1}{2})}{\kappa^{3/2}(\kappa+1)} \times\frac{{}_2F_1[1,-\kappa;\kappa+2;-(1-\xi/i\sqrt{\kappa})/(1+\xi/i\sqrt{\kappa})]}{1+\xi/i\sqrt{\kappa}}. \quad \text{(A8)}$$

In arriving at (A8) we have used the fact that ${}_2F_1[\kappa+1,0;-\kappa;z]=1$. Equation (17) results from (A8) upon using the relation[18]

$$ {}_2F_1[a,b;c;z]=(1-z)^{-a}{}_2F_1[a,c-b;c;-z/(1-z)].$$

[1] B. D. Fried and S. D. Conte, *The Plasma Dispersion Function* (Academic, New York, 1961).
[2] A. Achterberg and C. A. Norman, Astron. Astrophys. **89**, 353 (1980).
[3] W. C. Feldman, B. Abraham-Shrauner, J. R. Asbridge, and S. J. Bame, in *Physics of the Solar Planetary Environments*, edited by D. J. Williams (American Geophysical Union, Washington, DC, 1976), p. 413.
[4] F. C. Jones and D. C. Ellison, Space Sci. Rev. **58**, 259 (1991).
[5] A. Hasegawa, K. Mima, and M. Duong-van, Phys. Rev. Lett. **54**, 2608 (1985).
[6] M. Scholer, Geophys. Res. Lett. **17**, 1821 (1990).
[7] M. Scholer and T. Terasawa, Geophys. Res. Lett. **17**, 119 (1990).
[8] H. Kucharek and M. Scholer, J. Geophys. Res. **96**, 21 195 (1991).
[9] R. L. Mace and F. C. Jones, "Relativistic, parallel and quasi-parallel shocks in pair plasmas: Particle acceleration," submitted to Astrophys. J.
[10] R. M. Thorne and D. Summers, Phys. Fluids B **3**, 2117 (1991).
[11] Z. Meng, R. M. Thorne, and D. Summers, J. Plasma Phys. **47**, 445 (1992).
[12] H. Fichtner and S. R. Sreenivasan, J. Plasma Phys. **49**, 101 (1993).
[13] L. O'C Drury, Rep. Prog. Phys. **46**, 973 (1983).
[14] R. Blandford and D. Eichler, Phys. Rep. **154**, 1 (1987).
[15] D. B. Melrose, *Instabilities in Space and Laboratory Plasmas* (Cambridge University Press, Cambridge, 1986), pp. 134, 244–246.
[16] D. Summers and R. M. Thorne, Phys. Fluids B **3**, 1835 (1991).
[17] S. P. Christon, D. G. Mitchell, D. J. Williams, L. A. Frank, C. Y. Huang, and T. E. Eastman, J. Geophys. Res. **93**, 2562 (1988).
[18] N. Abramowitz and I. A. Stegun, *Handbook of Mathematical Functions* (Dover, New York, 1965), pp. 556–566.
[19] P. M. Morse and H. Feshbach, *Methods of Theoretical Physics* (McGraw-Hill, New York, 1953), Vol. 1, p. 424.
[20] L. J. Slater, *Generalized Hypergeometric Functions* (Cambridge University Press, Cambridge, 1966), pp. 3, 13–15, and 32.
[21] N. A. Krall and A. W. Trivelpiece, *Principles of Plasma Physics* (McGraw-Hill, New York, 1973), p. 373.
[22] B. Abraham-Shrauner and W. C. Feldman, J. Plasma Phys. **17**, 123 (1977).
[23] W. H. Press, B. P. Flannery, S. A. Teukolsky, and W. T. Vetterling, *Numerical Recipes: The Art of Scientific Computing*, 2nd ed. (Cambridge University Press, Cambridge, 1992), pp. 208–211 and 271–273.